

A unified clumped isotope thermometer calibration (0.5–1100°C) using carbonate-based standardization

N.T. Anderson^{1*}, J.R. Kelson², S. Kele³, M. Daëron⁴, M. Bonifacie⁵, J.
Horita⁶, T.J. Mackey⁷, C.M. John⁸, T. Kluge⁹, P. Petschnig¹¹, A.B. Jost¹,
K.W. Huntington¹⁰, S.M. Bernasconi¹¹, K.D. Bergmann¹

¹Department of Earth, Atmospheric, and Planetary Sciences, Massachusetts Institute of Technology,
Cambridge, MA, 02135

²Department of Earth and Environmental Sciences, University of Michigan, Ann Arbor, MI 48109

³Institute for Geological and Geochemical Research, Research Centre for Astronomy and Earth Sciences,
1112 Budapest, Hungary

⁴Laboratoire des Sciences du Climat et de l'Environnement, LSCE/IPSL, CEA-CNRS-UVSQ, Université
Paris-Saclay, Orme des Merisiers, F-91191, Gif-sur-Yvette Cedex, France

⁵Institut de Physique du Globe de Paris, Sorbonne Paris Cité, Université Paris Diderot, UMR 7154
CNRS, F-75005 Paris, France

⁶Department of Geosciences, Texas Tech University, Lubbock, TX, 79409

⁷Department of Earth and Planetary Sciences, University of New Mexico, Albuquerque, NM, 87131

⁸Department of Earth Science and Engineering, Imperial College, Prince Consort Rd, London SW7 2AZ

⁹Institute of Applied Geosciences, Karlsruhe Institute of Technology, Adenauerring 20b, 76131 Karlsruhe,
Germany

¹⁰Department of Earth and Space Sciences and Quaternary Research Center, University of Washington,
Seattle, WA, USA

¹¹Geological Institute, ETH Zürich, CH-8092 Zürich, Switzerland

Key Points:

- Reanalysis of previous Δ_{47} calibration samples reconciles their discrepancies.
- No statistically significant difference is observed across a wide range of temperature and sample character.
- This Δ_{47} calibration is near-identical to a suite of recent calibrations using carbonate-based standardization.

*77 Massachusetts Ave., Cambridge, MA 02139

Corresponding author: N.T. Anderson, nanderso@mit.edu

Abstract

29 The potential for carbonate clumped isotope thermometry to independently constrain
30 both the formation temperature ($T_{\Delta_{47}}$) of carbonate minerals and fluid oxygen isotope
31 composition allows insight into long-standing questions in the Earth sciences, but remain-
32 ing discrepancies between calibration schemes hamper interpretation of $T_{\Delta_{47}}$ measure-
33 ments. To address discrepancies between calibrations, we designed and analyzed a sam-
34 ple suite (41 total samples) with broad applicability across the geosciences, with an ex-
35 ceptionally wide range of formation temperatures, precipitation methods, and mineralo-
36 gies. We see no statistically significant offset between sample types, although compar-
37 ison of calcite and dolomite remains inconclusive. When data are reduced identically, the
38 regression defined by this study is nearly identical to that defined by four previous cal-
39 ibration studies that used carbonate-based standardization; we combine these data to
40 present a composite carbonate-standardized regression equation. Agreement across a wide
41 range of temperature and sample types demonstrates a unified, broadly applicable clumped
42 isotope thermometer calibration.
43

Plain Language Summary

44 Carbonate clumped isotope thermometry is a geochemical tool used to determine
45 the formation temperature of carbonate minerals. In contrast to previous carbonate ther-
46 mometers, clumped isotope thermometry requires no assumptions about the isotopic com-
47 position of the fluid from which the carbonate precipitated. By measuring the clumped
48 isotope composition (Δ_{47}) of carbonate minerals with a known formation temperature,
49 we can construct an empirical calibration for the clumped isotope thermometer that is
50 necessary to convert from a Δ_{47} value to formation temperature. Many previous stud-
51 ies have created Δ_{47} temperature calibrations, but differences between calibrations have
52 led to large uncertainty in final Δ_{47} temperatures. This study measures a large number
53 of samples that span a wide range of temperature (0.5–1100°C) and include many dif-
54 ferent types of carbonates. These data show that a single calibration equation can de-
55 scribe many sample types, and that when data are carefully standardized to a common
56 set of carbonate materials, calibrations performed at different laboratories agree almost
57 identically. We combine these data to present a carbonate clumped isotope thermome-
58 ter calibration with broad applicability across the geosciences.
59

1 Introduction

Carbonate clumped isotope thermometry is a powerful geochemical tool that can determine the formation temperature of a carbonate mineral based on the temperature-dependent propensity for ^{13}C - ^{18}O bond formation in the carbonate crystal lattice (Schauble et al., 2006). By reacting carbonate minerals with acid and measuring the resultant quantity of mass-47 CO_2 molecules (δ^{47} ; a value primarily controlled by the abundance ^{13}C - ^{18}O - ^{16}O in the analyzed CO_2) and comparing it to a stochastic distribution of ^{13}C - ^{18}O - ^{16}O CO_2 with the same "bulk" isotopic composition ($\delta^{18}\text{O}$, $\delta^{13}\text{C}$), the excess abundance of the doubly substituted isotopologue (Δ_{47}) can be calculated (Ghosh et al., 2006; Schauble et al., 2006). Because Δ_{47} reflects an internal state of isotope distribution within the carbonate mineral phase, it can be used to calculate mineral formation temperature ($T_{\Delta_{47}}$) as well as the $\delta^{18}\text{O}$ of the precipitating fluid. This duo can be leveraged to inform long-standing questions across many geoscience disciplines, including the temperature history of the Earth's oceans, terrestrial paleotemperature, diagenetic history of carbonates, and, when coupled to chronology proxies, basin thermochronology (Finnegan et al., 2011; Snell et al., 2013; Winkelstern & Lohmann, 2016; Lloyd et al., 2017; Mangenot et al., 2018).

The calibration between Δ_{47} and carbonate mineral formation temperature is a key intermediary between measurement of CO_2 gas on a mass spectrometer and calculation of $T_{\Delta_{47}}$. Many laboratories have produced T - Δ_{47} calibrations since the initial study of Ghosh et al. (2006), spanning various temperatures, mineralogies, precipitation methods, analytical techniques, and data processing procedures (e.g., Ghosh et al., 2006; Eiler, 2007; Dennis et al., 2011; Kele et al., 2015; Kelson et al., 2017; Bonifacie et al., 2017; Bernasconi et al., 2018; Jautzy et al., 2020). While early attempts to compare empirical calibration studies across laboratories yielded large discrepancies (e.g., Ghosh et al., 2006; Dennis & Schrag, 2010), recent calibration studies have converged on statistically similar slopes for the T - Δ_{47} regression line when data is reduced consistently (Petersen et al., 2019). The convergence of these calibrations is promising, but current discrepancies between empirical calibration equations still lead to $T_{\Delta_{47}}$ differences of ~ 10 °C for carbonates near Earth surface temperatures and tens of °C for higher temperature samples (Fig. 1; Petersen et al., 2019; Jautzy et al., 2020). Uncertainty from calibrations on this order compounds with analytical uncertainty and hampers interpretation of clumped isotope data.

91 The source of discrepancy between calibration efforts remains unclear. By repro-
92 cessing past calibration data with a consistent data reduction scheme and IUPAC pa-
93 rameter set (Brand et al., 2010; Daéron et al., 2016; Schauer et al., 2016), Petersen et
94 al. (2019) reduced but did not eliminate differences between calibrations. Remaining off-
95 set in calibration schemes was attributed to one or more of the following: carbon diox-
96 ide equilibrium scale (CDES) standardization scheme (heated/equilibrated gas vs. carbonate-
97 based standardization; number, composition, and distribution of standards), differences
98 in the concentration, temperature, and application method of orthophosphoric acid, sam-
99 ple gas purification procedures, mass spectrometer methods, pressure baseline correc-
100 tion, and kinetic isotope effects during carbonate precipitation (Petersen et al., 2019).

101 The 'InterCarb' carbonate clumped isotope inter-laboratory comparison project,
102 following the principle of equal sample/standard treatment, demonstrated that using car-
103 bonate standards (as opposed to heated/equilibrated gases) to project raw Δ_{47} values
104 into the 'I-CDES' yields reproducibility between 25 laboratories neither greater nor smaller
105 than predicted based on fully propagating intra-laboratory analytical uncertainties (Bernasconi
106 et al., submitted; Daéron, submitted). Furthermore, the InterCarb study found that Δ_{47}
107 values of measured carbonate standards are statistically indistinguishable irrespective
108 of procedural differences between laboratories such as sample gas purification, mass spec-
109 trometer type, or sample acidification procedure. Jautzy et al. (2020) created a new cal-
110 ibration spanning 5–726°C using carbonate-based standardization, and found the regres-
111 sion equation defined by the data was statistically indistinguishable from a series of pre-
112 vious calibration efforts using carbonate-based standardization (Peral et al., 2018; Bernasconi
113 et al., 2018; Breitenbach et al., 2018; Piasecki et al., 2019; Daéron et al., 2019; Meinicke
114 et al., 2020). Together, these studies support that varying preparation and measurement
115 procedures between laboratories produce consistent results if data are standardized us-
116 ing common carbonate reference materials.

117 Given the promising inter-laboratory consistency of the InterCarb project (Bernasconi
118 et al., submitted), a new calibration encompassing a spectrum of carbonates relevant to
119 geoscience researchers that is firmly anchored to the I-CDES using carbonate-based stan-
120 dardization is required. To ensure that this calibration is applicable across a wide range
121 of sample material, we reanalyzed a sample suite consisting of natural and synthetic sam-
122 ples measured from four previously discrepant calibration efforts (Kele et al., 2015; Kluge
123 et al., 2015; Bonifacie et al., 2017; Kelson et al., 2017) and analyzed a new suite of low-

124 temperature lacustrine carbonates from the Dry Valleys, Antarctica and experimentally
125 heated carbonate standards. This sample suite spans broad ranges in temperature (0.5
126 – 1100°C), precipitation method (active degassing, passive degassing, mixed solution, nat-
127 ural precipitation), mineralogy (calcite, dolomite, and minor aragonite), and initial bulk
128 isotopic composition. In accordance with the suggestions of the InterCarb project, the
129 latest anchor values for carbonate standards (ETH-1–4, MERCK, IAEA-C2) were used
130 for carbonate-based standardization, measurement of each sample was replicated at least
131 six times (mean = 9), sample to standard ratio was 1:1, IUPAC parameters were used
132 to correct raw data, and analytical uncertainty and uncertainty associated with creation
133 of the reference frame was propagated throughout. We compare the regression derived
134 by data presented here to a suite of previous studies using carbonate-based standard-
135 ization (recalculated with InterCarb anchor values), and combine these datasets to pro-
136 pose a unified and broadly applicable clumped isotope thermometer calibration.

137 2 Materials and Methods

138 2.1 Sample collection and preparation

139 A total of 41 carbonate samples with known precipitation temperatures from four
140 previous calibration efforts (Kele et al., 2015; Kluge et al., 2015; Bonifacie et al., 2017;
141 Kelson et al., 2017), a suite of Antarctic lacustrine carbonate, and a suite of experimen-
142 tally heated ETH standards were (re)analyzed in this study. Sample formation temper-
143 ature ranges from 0.5–1100°C. Three samples are stoichiometric dolomite, one sample
144 is non-stoichiometric proto-dolomite, one sample is aragonite (with minor calcite) and
145 the remainder are calcite (five with minor aragonite; one with minor goethite).

146 2.1.1 *Natural precipitates*

147 Six calcite samples were collected from three perennially ice-covered lakes in the Dry
148 Valleys region of Antarctica: two samples from Lake Fryxell (see Jungblut et al., 2016),
149 three from Lake Joyce (see Mackey et al., 2018), and one from Lake Vanda (see Mackey
150 et al., 2017). These carbonates precipitated in association with microbial mats and are
151 shown by previous work to have extremely low $\delta^{18}\text{O}$ values of -30 to -40‰ (Mackey
152 et al., 2018).

153 Ten tufa and travertine deposits were sampled from central Italy, Hungary, Yun-
154 nan Province (China), Yellowstone (USA), and Tenerife (Spain). Detailed description
155 of sample localities and strategy are given in Kele et al. (2015) and references therein.

156 **2.1.2 Laboratory precipitates**

157 Aliquots of ETH-1 (Carrara marble) and ETH-2 (synthetic carbonate) were heated
158 to 1100°C and pressurized to 2000 bar for a period of 24 hours at the ETH Zürich Rock
159 Deformation Laboratory. Following heating, samples were quenched to room tempera-
160 ture within seconds. See Text S1 in the supporting information for full methods.

161 Fifteen calcite samples from Kelson et al. (2017) were either precipitated with so-
162 lutions of NaHCO₃ and CaCl₂ or by dissolving CaCO₃ in H₂O with low pH from CO₂
163 bubbling, and then inducing precipitation either through N₂ bubbling or passive degassing.
164 Carbonic anhydrase was added to four samples. Temperature precision was ±0.5°C.

165 Two calcite samples from Kluge et al. (2015) were precipitated by dissolving CaCO₃
166 in H₂O and letting the solution equilibrate for 2–15 hours, filtering out undissolved car-
167 bonate, and bubbling CO₂ through the solution.

168 Four (proto)dolomite samples used in this study were originally described in Horita
169 (2014) and Bonifacie et al. (2017). The 80°C sample was precipitated by mixing MgSO₄,
170 Ca(NO₃)₄H₂O, and Na₂CO₃ in a sealed glass bottle held within 1°C of nominal temper-
171 ature for 41 days. The 100, 250, and 350°C samples were made by mixing ground nat-
172 ural aragonite or calcite with a Ca-Mg-(Na)-Cl solution and held within 2°C of prescribed
173 value for 6–85 days.

174 **2.2 Mass spectrometry**

175 **2.2.1 This study**

176 Sample Δ_{47} was measured from January 2018 to November 2020 at the MIT Car-
177 bonate Research Laboratory on a Nu Perspective dual-inlet isotope ratio mass spectrom-
178 eter with a NuCarb automated sample preparation unit held at 70°C (see Mackey et al.,
179 2020). Carbonate samples (including dolomite) weighing 400–600 μg reacted for 25 min-
180 utes in individual glass vials with 150 μl orthophosphoric acid ($\rho = 1.93 \text{ g/cm}^3$). Evolved
181 CO₂ gas was purified cryogenically and by passive passage through a Porapak trap (1/4”

Table 1. Description of analyzed and reanalyzed samples.

Study	Mineralogy	Formation	Formation	Samples
			Temp. Range (°C) ^a	Analyzed (this study; orig. study)
Bonifacie et al. (2017)	Dolo., proto-dolo.	Mixed solution	80–350	4; 12
Kele et al. (2015)	Calc. (minor arag.)	Tufa, travertine	5–95	12; 24
Kelson et al. (2017)	Calc. (minor arag.)	Active/passive degas, mixed sol'n	6–78	15; 56
Kluge et al. (2015)	Calc., arag.	Active degas	25–80	2; 29
This study	Calc.	Lacustrine, experimentally heated	0.5–1100	8

^aTemperature range is only for samples reanalyzed in this study.

182 ID; 0.4 g 50/80 mesh Porapak Q) held at -30°C. Purified sample gas and reference gas
 183 of known composition were alternately measured on six Faraday collectors (m/z 44–49)
 184 in 3 acquisitions of 20 cycles, each with 30 second integration time (30 minute total in-
 185 tegration time). Initial voltage was 8–20 V on the m/z 44 beam with $2e^8 \Omega$ resistors and
 186 depleted by approximately 50% over the course of an analysis. Sample and standard gases
 187 depleted at equivalent rates from microvolumes over the integration time.

188 Each run of approximately 50 individual analyses began with each of ETH-1–ETH-
 189 4 in random order, and then alternated between blocks of three unknowns and two ETH
 190 anchors. Additionally, IAEA-C1, IAEA-C2, and MERCK were respectively measured
 191 once per run. Unknown to anchor ratio was planned at 1:1 for each run, although gas
 192 preparation or mass spectrometer error occasionally modified this ratio. The reference
 193 side of the dual-inlet was refilled with reference gas every 10 to 17 analyses. In total, un-
 194 knowns were measured 6–16 times over the study interval (362 total unknown analyses).

195 2.3 Data processing

196 Raw mass spectrometer data were first processed by removing cycles (i.e., single
 197 integration cycles of mass spectrometer measurement) with raw Δ_{47} values more than
 198 5 "long-term" standard deviations (the mean of the respective cycle-level SD for ETH-
 199 1–4 over a 3-month period, 0.10%) away from the median Δ_{47} measurement for the anal-

200 ysis. Analyses with more than 20 cycles (out of 60 total cycles) falling outside the 5 long-
 201 term SD threshold were removed. In total, 0.81% of cycles and 0.42% of analyses were
 202 removed. No pressure baseline correction was applied. Long-term repeatability (1SD)
 203 of Δ_{47} for all analyses (after data processing described above) is 0.036 ‰.

204 After cycle-level outlier removal, data were processed using the 'D47crunch' Python
 205 package (Daëron, submitted) using IUPAC ^{17}O parameters, 70°C ^{18}O acid fractionation
 206 factor of 1.00871 (Kim et al., 2007), and projected to the I-CDES with values for ETH-
 207 1–4, IAEA-C2, and MERCK from the InterCarb exercise (Bernasconi et al., submitted),
 208 which uses a 90°C acid fractionation factor of -0.088‰ from Petersen et al. (2019). Raw
 209 Δ_{47} measurements were converted to the I-CDES using a pooled regression approach that
 210 accounts for the relative mapping of all samples in δ^{47} - Δ_{47} space (Daëron, submitted).
 211 Analytical uncertainty and error associated with creation of the reference frame were fully
 212 propagated through the dataset. A full description of the data reduction procedure used
 213 in D47crunch is detailed in (Daëron, submitted). Each run (typically 50 analyses) was
 214 treated as an analytical session. IAEA-C1 was treated as an unknown and used as an
 215 internal consistency check (mean = 0.291‰, 1SE = 0.01‰). Finally, Peirce's criterion
 216 (Ross, 2003; Zaarur et al., 2013) was applied to the dataset at the analysis level; a to-
 217 tal of six analyses were marked as outliers and removed, followed by reprocessing of the
 218 dataset.

219 **3 Results and Discussion**

220 Results for all analyses (re)analyzed here are summarized at the sample level in Ta-
 221 ble 2 (see Dataset S1 and S2 for full results). Accounting for uncertainty in Δ_{47} (long-
 222 term repeatability, 1SD) and formation temperature (0.5–10°C) with the regression method
 223 described in York et al. (2004), these data define a linear $1/T^2$ - Δ_{47} relationship from 0.5°C–
 224 1100°C shown in Figure 1.

225 **3.1 Comparison of T- Δ_{47} relationship across sample types**

226 The published regression equations from Kele et al. (2015); Kluge et al. (2015); Kel-
 227 son et al. (2017); Bonifacie et al. (2017) all fall within the 95% confidence interval of the
 228 regressions defined by this study's reanalysis of their constituent samples (supporting
 229 information Fig. S3). Natural and lab-precipitated samples fall on nearly identical re-

gression lines (Fig. 2A); analysis of covariance (ANCOVA) fails to reject the null hypothesis that both types of samples are characterized by a single regression line at the 95% confidence level at our typical sample precision levels (1SE) of ~ 10 ppm ($p_{slope} = 0.41$, $p_{intercept} = 0.19$; see Table S1 in supporting information for full table of ANCOVA analyses). Natural samples display a weaker correlation coefficient ($r^2 = 0.96$ vs. 0.99) and larger error of the estimate, likely due to variable fluid temperatures in natural settings.

Our reanalysis of samples precipitated by Kelson et al. (2017) supports their conclusions: we observe no statistically significant Δ_{47} offset between passively and actively degassed samples ($p_{slope} = 0.19$, $p_{intercept} = 0.79$) or with the addition of carbonic anhydrase ($p_{slope} = 0.79$, $p_{intercept} = 0.32$; Fig. S1). Reanalysis of samples from Kele et al. (2015) and Kelson et al. (2017) confirms the results of Kele et al. (2015) in that there is no significant difference between samples precipitated at low (< 7) vs. high (> 7) pH ($p_{slope} = 0.4$, $p_{intercept} = 0.99$) or intensive vs. moderate precipitation rate ($p_{slope} = 0.12$, $p_{intercept} = 0.54$; Fig. S2). The low number of rapid precipitates (particularly at low temperatures) makes this claim inconclusive, but Δ_{47} values for two extremely slow-growing samples measured for this study on an Isoprime 100 dual-inlet mass spectrometer located at LCSE (methods in supporting information Text S3), respectively from Devil’s Hole, NV, USA, and Laghetto Basso, Italy (see Winograd et al., 2006; Coplen, 2007; Drysdale et al., 2012; Daëron et al., 2019), are nearly identical to the expected values based on the calibration from this study (Fig. 3B). Calcite-water fractionation in ^{18}O calculated from a subset of 20 samples with fluid $\delta^{18}\text{O}$ data (Fig. S5) agrees closely with the equations of Coplen (2007) and Daëron et al. (2019). The Antarctic microbially-mediated lacustrine calcites show no discernible offset from the overall trend, but small sample numbers and limited temperature range prohibit formal analysis.

With only three stoichiometric dolomite samples, no stoichiometric dolomite samples below 100°C , and no calcite samples between 95°C and 1000°C measured for this study, we cannot rigorously compare calcite and dolomite regressions; ANCOVA variably accepts/rejects the null hypothesis depending on categorization of the single protodolomite sample. We tentatively assert that dolomite and calcite samples can be described using a single regression equation, as previously suggested by Bonifacie et al. (2017) and Petersen et al. (2019), but analysis of dolomite samples with lower ($< 80^\circ\text{C}$) and higher ($> 350^\circ\text{C}$) formation temperature is needed to confirm this claim. The regression through aragonitic samples (four samples $< 6\%$; one sample = 38% ; one sample = 78%) is statistically

263 similar to the regression through all calcite samples (Fig. 2B). A single sample (Aqua
264 Borra) with minor goethite (15%) has individual Δ_{47} analyses both much higher and lower
265 than expected, but has a mean Δ_{47} value that closely agrees with the regression pres-
266 ened here.

267 The absence of systematic offset in T- Δ_{47} relationship corresponding to any known
268 sample characteristic suggests that discrepancies between these exact samples from pre-
269 vious calibration efforts are not a product of the character of measured sample material
270 (Wacker et al., 2014; Kele et al., 2015; Kluge et al., 2015; Kelson et al., 2017; Bonifacie
271 et al., 2017). Furthermore, the consistency of the T- Δ_{47} relationship across a broad range
272 of materials and temperatures (e.g., from Antarctic lacustrine microbially-mediated car-
273 bonates to laboratory-grown carbonates heated to 1100°C) indicates that a single T- Δ_{47}
274 calibration can adequately describe a wide variety of sample types.

275 **3.2 Comparison across calibration studies using carbonate-based stan-** 276 **dardization**

277 Reprocessing data from the synthetic calcite calibration of Jautzy et al. (2020), as
278 well as a suite of foraminifera-based calibration studies (Breitenbach et al., 2018; Peral
279 et al., 2018; Meinicke et al., 2020) with updated InterCarb anchor values (Bernasconi
280 et al., submitted) yields an almost identical regression to that calculated in this study
281 (Fig. 3). The near-perfect agreement of these calibrations ($\sim 0.5^\circ\text{C}$ offset near 25°C ; $\sim 2^\circ\text{C}$
282 offset near 100°C) despite differences in sample material and measurement method points
283 to the strength of carbonate-based standardization and the potential of a unified clumped
284 isotope calibration.

285 This clumped isotope calibration covers the broadest range of temperatures, includes
286 diverse carbonates, replicates measurements several times, and uses a low unknown:anchor
287 ratio to firmly tie unknown measurements to the I-CDES. However, this calibration has
288 an unequal distribution of samples in $1/T^2$ space, is anchored at the coldest tempera-
289 tures by unusual carbonates, and does not contain marine carbonates, which are of par-
290 ticular interest to the clumped isotope community. To address these weaknesses, we com-
291 bine data from this study with four other carbonate-standardized calibrations (Breitenbach
292 et al., 2018; Peral et al., 2018; Meinicke et al., 2020; Jautzy et al., 2020) to present a com-
293 posite $1/T^2$ - Δ_{47} regression that has smaller temperature gaps, is anchored at low tem-

294 peratures by a variety of samples, and extends the calibration to biogenic marine car-
 295 bonates:

$$\Delta_{47(I-CDES90^{\circ}C)} = 0.0390 \pm 0.0004 \times \frac{10^6}{T^2} + 0.153 \pm 0.004 \quad (r^2 = 0.97) \quad (1)$$

296 Along with excellent agreement between laboratories using carbonate-based stan-
 297 dardization, this dataset and the community-developed InterCarb anchor values (Bernasconi
 298 et al., submitted) narrow the discrepancy between calibrations using carbonate anchor
 299 values and heated/equilibrated gases, most notably Petersen et al. (2019). Specifically,
 300 calibrations of Jautzy et al. (2020) and Petersen et al. (2019) differed by 5°C near 25°C
 301 and 20°C near 100°C; the composite calibration regression shown in Equation 1 differs
 302 from Petersen et al. (2019) by 3°C near 25°C and by 7°C near 100°C (Fig. 1A).

303 **3.3 Non-linearity of $1/T^2$ - Δ_{47} relationship for high-temperature pre-** 304 **cipitates**

305 At high temperatures, theory predicts a non-linear $1/T^2$ - Δ_{47} relationship (e.g., Guo
 306 et al., 2009; Hill et al., 2014), which is supported by recent empirical calibrations (e.g.,
 307 Müller et al., 2019; Jautzy et al., 2020). A third-order polynomial regression through our
 308 data falls within the 95% CL of our linear fit over the entire temperature range (Fig. 3A)
 309 and does not improve the goodness of fit ($r^2 = 0.97$ for both); we observe no evidence
 310 that a non-linear fit better describes high-temperature data.

311 **4 Conclusions**

312 When measured in a consistent analytical setting with carbonate-based standard-
 313 ization, no systematic offset is observed between samples precipitated across a broad spec-
 314 trum of conditions that were previously determined to have disparate Δ_{47} values. Among
 315 sample types measured here, we find no evidence that the particular character of sam-
 316 ple material (e.g., mineralogy, addition of carbonic anhydrase, pH, precipitation rate, bi-
 317 ological mediation) influences the Δ_{47} calibration, although our tentative claim of cal-
 318 cite and dolomite agreement remains inconclusive.

319 Furthermore, when anchor values from the InterCarb exercise (Bernasconi et al.,
 320 submitted) are used to correct all data with data reduction best practices (Petersen et

Table 2. Final corrected $\delta^{13}\text{C}_{VPDB}$ (‰), $\delta^{18}\text{O}_{VSMOW}$ (‰), and $\Delta_{47(CDES90^\circ\text{C})}$ (‰) results.

Sample name	Author	Mineralogy	Method	T(°C)	N	$\delta^{13}\text{C}$	$\delta^{18}\text{O}$	Δ_{47}	SE	95% CL
IPGP_100-A3	Bonifacie	Dolomite	Lab	102.3	9	-46.3	-17.4	0.425	0.015	0.029
IPGP_250-A5	Bonifacie	Dolomite	Lab	252.1	9	-52.8	-28.0	0.272	0.025	0.049
IPGP_350-A9	Bonifacie	Dolomite	Lab	351.4	10	-55.6	-32.0	0.229	0.018	0.035
IPGP_80-1	Bonifacie	Proto-dolo.	Lab	80.2	10	-6.9	-16.2	0.494	0.012	0.024
ETH-1-1100-SAM	This study	Calcite	Lab	1100	10	2.0	-2.0	0.177	0.018	0.036
ETH-2-1100-SAM	This study	Calcite	Lab	1100	10	-10.1	-18.4	0.190	0.017	0.034
HT_25C	Kluge	Calcite	Lab	25	9	2.1	-6.2	0.609	0.013	0.026
HT_80C	Kluge	Aragonite	Lab	80	9	1.1	-15.4	0.486	0.013	0.025
AQUA.BORRA	Kele	Calcite	Natural	36.1	11	1.7	-8.4	0.576	0.012	0.023
BUK_4	Kele	Calcite	Natural	54.9	9	2.2	-15.0	0.539	0.013	0.025
CANARIAN	Kele	Calcite	Natural	33.8	8	0.1	-10.2	0.583	0.014	0.027
CANNATOPA	Kele	Calcite	Natural	11	8	-4.1	-5.4	0.627	0.014	0.027
IGAL	Kele	Calcite	Natural	75	10	0.6	-13.5	0.474	0.012	0.024
LAPIGNA	Kele	Calcite	Natural	12.5	9	-11.4	-5.5	0.620	0.013	0.026
NG_2	Kele	Calcite	Natural	60.4	9	3.6	-24.6	0.504	0.013	0.025
P5-SUMMER	Kele	Calcite	Natural	12	9	5.4	-14.3	0.632	0.013	0.026
P5-WINTER	Kele	Calcite	Natural	5	10	5.1	-12.7	0.635	0.013	0.026
SARTEANO	Kele	Calcite	Natural	20.7	9	0.4	-7.3	0.593	0.013	0.025
SZAL-2	Kele	Calcite	Natural	11	9	-10.3	-8.2	0.653	0.013	0.026
TURA	Kele	Calcite	Natural	95	9	3.7	-23.2	0.408	0.013	0.025
LF2012-9-7-A	This study	Calcite	Natural	2.5	4	2.6	-27.2	0.662	0.023	0.045
LF2012-D1-A	This study	Calcite	Natural	2.5	4	3.4	-27.1	0.656	0.023	0.044
LJ2010-12A-Z1A	This study	Calcite	Natural	0.5	13	7.7	-39.4	0.667	0.014	0.028
LJ2010-12A-Z2A	This study	Calcite	Natural	0.5	6	8.1	-38.1	0.671	0.020	0.039
LJ2010-5B-A	This study	Calcite	Natural	0.5	11	8.1	-37.6	0.674	0.014	0.027
LV26NOV10-2A	This study	Calcite	Natural	4	6	11.2	-29.0	0.651	0.018	0.035
UWCP14.20C_9	Kelson	Calcite	Lab	23	8	-21.1	-10.8	0.603	0.014	0.028
UWCP14.20C_CA_11	Kelson	Calcite	Lab	23	10	-14.1	-10.9	0.614	0.013	0.025
UWCP14.21C_1	Kelson	Calcite	Lab	22	8	-18.6	-11.1	0.609	0.014	0.028
UWCP14.4C_3	Kelson	Calcite	Lab	6	8	-21.3	-6.6	0.648	0.014	0.028
UWCP14.4C_4	Kelson	Calcite	Lab	6	9	-23.4	-6.7	0.657	0.013	0.026
UWCP14.50C_2	Kelson	Calcite	Lab	51	9	-18.4	-16.4	0.533	0.013	0.026
UWCP14.50C_7	Kelson	Calcite	Lab	54	9	-0.2	-17.4	0.517	0.013	0.025
UWCP14.50C_CA_11	Kelson	Calcite	Lab	50	9	-18.5	-15.9	0.526	0.014	0.027
UWCP14.60C_2	Kelson	Calcite	Lab	66	9	-12.5	-18.2	0.489	0.013	0.026
UWCP14.70C_4	Kelson	Calcite	Lab	72	8	-17.7	-18.8	0.488	0.014	0.028
UWCP14.70C_CA_4	Kelson	Calcite	Lab	71	9	-0.2	-19.6	0.491	0.013	0.025
UWCP14.80C_2	Kelson	Calcite	Lab	78	9	-6.9	-20.9	0.482	0.013	0.025
UWCP14.8C_2	Kelson	Calcite	Lab	9	9	-15.1	-7.7	0.632	0.013	0.026
UWCP14.8C_6	Kelson	Calcite	Lab	9	9	0.4	-8.8	0.647	0.013	0.026
UWCP14.8C_CA_4	Kelson	Calcite	Lab	9	8	-17.4	-8.1	0.647	0.014	0.028

al., 2019; Daëron, submitted), the $1/T^2$ - Δ_{47} regression defined by data presented here is nearly identical (0.5°C offset at 25°C; 2°C offset at 100°C) to the regression defined by a suite of recent calibration studies (Peral et al., 2018; Breitenbach et al., 2018; Meinicke et al., 2020; Jautzy et al., 2020) and closely approximates the composite calibration of Petersen et al. (2019). Equation 1 spans the broadest range of temperatures measured in a consistent analytical setting and, when corrected with carbonate anchor values from the InterCarb exercise (Bernasconi et al., submitted) or heated/equilibrated gases, may be applied across a wide range of natural and laboratory-grown carbonate material.

Acknowledgments

Regression equations from previous publications are included in cited papers. Sample and replicate level data are included in this manuscript in the supporting information and will be archived in the EarthChem database using a data template specifically designed for carbonate clumped isotope data (Petersen et al., 2019) pending acceptance of this manuscript. N.T. Anderson acknowledges the support of the J.H. and E.V. Wade Fellowship and the mTerra Catalyst Fund. Members of the Bergmann Lab (Marjorie Cantine, Athena Eyster, Sam Goldberg, and Julia Wilcots) provided helpful feedback on early drafts. K. Bergmann acknowledges support from the Packard Foundation, NASA Exobiology Grant 80NSSC19K0464 and the MIT Wade Fund.

References

- Bernasconi, S. M., Daëron, M., Bergmann, K. D., Bonifacie, M., Meckler, A. N., Affek, H. P., ... Ziegler, M. (submitted). InterCarb: A community effort to improve inter-laboratory standardization of the carbonate clumped isotope thermometer using carbonate standards. *Geochemistry, Geophysics, Geosystems*. doi: 10.1002/essoar.10504430.4
- Bernasconi, S. M., Müller, I. A., Bergmann, K. D., Breitenbach, S. F., Fernandez, A., Hodell, D. A., ... Ziegler, M. (2018). Reducing uncertainties in carbonate clumped isotope analysis through consistent carbonate-based standardization. *Geochemistry, Geophysics, Geosystems*, 19(9), 2895–2914. doi: 10.1029/2017GC007385
- Bonifacie, M., Calmels, D., Eiler, J. M., Horita, J., Chaduteau, C., Vasconcelos, C., ... Bourrand, J. J. (2017). Calibration of the dolomite clumped isotope ther-

- 352 mometer from 25 to 350 °C, and implications for a universal calibration for all
353 (Ca, Mg, Fe)CO₃carbonates. *Geochimica et Cosmochimica Acta*, 200, 255–279.
354 doi: 10.1016/j.gca.2016.11.028
- 355 Brand, W. A., Assonov, S. S., & Coplen, T. B. (2010). Correction for the 17O
356 interference in $\delta^{13}\text{C}$ measurements when analyzing CO₂ with stable isotope
357 mass spectrometry (IUPAC Technical Report). *Pure Applied Chemistry*, 82(8),
358 1719–1733. doi: 10.1351/PAC-REP-09-01-05
- 359 Breitenbach, S. F., Mleneck-Vautravers, M. J., Grauel, A. L., Lo, L., Bernasconi,
360 S. M., Müller, I. A., ... Hodell, D. A. (2018). Coupled Mg/Ca and
361 clumped isotope analyses of foraminifera provide consistent water temper-
362 atures. *Geochimica et Cosmochimica Acta*, 236, 283–296. doi: 10.1016/
363 j.gca.2018.03.010
- 364 Coplen, T. B. (2007). Calibration of the calcite-water oxygen-isotope geothermome-
365 ter at Devils Hole, Nevada, a natural laboratory. *Geochimica et Cosmochimica*
366 *Acta*, 71(16), 3948–3957. doi: 10.1016/j.gca.2007.05.028
- 367 Daëron, M. (submitted). Full propagation of analytical uncertainties in D47
368 measurements. *Geochemistry, Geophysics, Geosystems*. doi: 10.1002/
369 essoar.10504430.4
- 370 Daëron, M., Blamart, D., Peral, M., & Affek, H. P. (2016). Absolute isotopic abun-
371 dance ratios and the accuracy of $\Delta 47$ measurements. *Chemical Geology*, 442,
372 83–96. doi: 10.1016/j.chemgeo.2016.08.014
- 373 Daëron, M., Drysdale, R. N., Peral, M., Huyghe, D., Blamart, D., Coplen,
374 T. B., ... Zanchetta, G. (2019). Most Earth-surface calcites precipitate
375 out of isotopic equilibrium. *Nature Communications*, 10(1), 1–7. doi:
376 10.1038/s41467-019-08336-5
- 377 Dennis, K. J., Affek, H. P., Passey, B. H., Schrag, D. P., & Eiler, J. M. (2011).
378 Defining an absolute reference frame for ‘clumped’ isotope studies of
379 CO₂. *Geochimica et Cosmochimica Acta*, 75(22), 7117–7131. Retrieved
380 from <http://dx.doi.org/10.1016/j.gca.2011.09.025> doi: 10.1016/
381 j.gca.2011.09.025
- 382 Dennis, K. J., & Schrag, D. P. (2010). Clumped isotope thermometry of carbon-
383 atites as an indicator of diagenetic alteration. *Geochimica et Cosmochimica*
384 *Acta*, 74(14), 4110–4122. doi: 10.1016/j.gca.2010.04.005

- 385 Drysdale, R. N., Paul, B. T., Hellstrom, J. C., Couchoud, I., Greig, A., Bajo, P.,
386 ... Woodhead, J. D. (2012). Precise microsampling of poorly laminated
387 speleothems for U-series dating. *Quaternary Geochronology*, *14*, 38–47. doi:
388 10.1016/j.quageo.2012.06.009
- 389 Eiler, J. M. (2007). "Clumped-isotope" geochemistry-The study of naturally-
390 occurring, multiply-substituted isotopologues. *Earth and Planetary Science*
391 *Letters*, *262*(3-4), 309–327. doi: 10.1016/j.epsl.2007.08.020
- 392 Finnegan, S., Bergmann, K., Eiler, J. M., Jones, D. S., Fike, D. A., Eisenman,
393 I., ... Fischer, W. W. (2011). The magnitude and duration of Late
394 Ordovician-Early Silurian glaciation. *Science*, *331*(6019), 903–906. doi:
395 10.1126/science.1200803
- 396 Ghosh, P., Adkins, J., Affek, H., Balta, B., Guo, W., Schauble, E. A., ... Eiler,
397 J. M. (2006). ^{13}C - ^{18}O bonds in carbonate minerals: A new kind of pale-
398 oothermometer. *Geochimica et Cosmochimica Acta*, *70*(6), 1439–1456. doi:
399 10.1016/j.gca.2005.11.014
- 400 Guo, W., Mosenfelder, J. L., Goddard, W. A., & Eiler, J. M. (2009). Isotopic
401 fractionations associated with phosphoric acid digestion of carbonate miner-
402 als: Insights from first-principles theoretical modeling and clumped isotope
403 measurements. *Geochimica et Cosmochimica Acta*, *73*(24), 7203–7225. doi:
404 10.1016/j.gca.2009.05.071
- 405 Hill, P. S., Tripathi, A. K., & Schauble, E. A. (2014). Theoretical constraints
406 on the effects of pH, salinity, and temperature on clumped isotope sig-
407 natures of dissolved inorganic carbon species and precipitating carbon-
408 ate minerals. *Geochimica et Cosmochimica Acta*, *125*, 610–652. doi:
409 10.1016/j.gca.2013.06.018
- 410 Horita, J. (2014). Oxygen and carbon isotope fractionation in the system dolomite-
411 water-CO₂ to elevated temperatures. *Geochimica et Cosmochimica Acta*, *129*,
412 111–124. doi: 10.1016/j.gca.2013.12.027
- 413 Jautzy, J., Savard, M., Dhillon, R., Bernasconi, S., Lavoie, D., & Smirnov, A.
414 (2020). Clumped isotope temperature calibration for calcite: Bridging the-
415 ory and experimentation. *Geochemical Perspective Letters*, *14*, 36–41. doi:
416 10.7185/geochemlet.2021
- 417 Jungblut, A. D., Hawes, I., Mackey, T. J., Krusor, M., Doran, P. T., Sumner, D. Y.,

- 418 ... Goroncy, A. K. (2016). Microbial mat communities along an oxygen gra-
419 dient in a perennially ice-covered Antarctic lake. *Applied and Environmental*
420 *Microbiology*, 82(2), 620–630. doi: 10.1128/AEM.02699-15
- 421 Kele, S., Breitenbach, S. F., Capezzuoli, E., Meckler, A. N., Ziegler, M., Millan,
422 I. M., ... Bernasconi, S. M. (2015). Temperature dependence of oxygen- and
423 clumped isotope fractionation in carbonates: A study of travertines and tufas
424 in the 6-95°C temperature range. *Geochimica et Cosmochimica Acta*, 168,
425 172–192. doi: 10.1016/j.gca.2015.06.032
- 426 Kelson, J. R., Huntington, K. W., Schauer, A. J., Saenger, C., & Lechler, A. R.
427 (2017). Toward a universal carbonate clumped isotope calibration: Di-
428 verse synthesis and preparatory methods suggest a single temperature
429 relationship. *Geochimica et Cosmochimica Acta*, 197, 104–131. doi:
430 10.1016/j.gca.2016.10.010
- 431 Kim, S. T., Mucci, A., & Taylor, B. E. (2007). Phosphoric acid fractionation fac-
432 tors for calcite and aragonite between 25 and 75 °C: Revisited. *Chemical Geol-*
433 *ogy*, 246(3-4), 135–146. doi: 10.1016/j.chemgeo.2007.08.005
- 434 Kluge, T., John, C. M., Jourdan, A. L., Davis, S., & Crawshaw, J. (2015). Labora-
435 tory calibration of the calcium carbonate clumped isotope thermometer in the
436 25-250°C temperature range. *Geochimica et Cosmochimica Acta*, 157, 213–227.
437 doi: 10.1016/j.gca.2015.02.028
- 438 Lloyd, M. K., Eiler, J. M., & Nabelek, P. I. (2017). Clumped isotope thermometry
439 of calcite and dolomite in a contact metamorphic environment. *Geochimica et*
440 *Cosmochimica Acta*, 197, 323–344. doi: 10.1016/j.gca.2016.10.037
- 441 Mackey, T. J., Jost, A. B., Creveling, J. R., & Bergmann, K. D. (2020). A Decrease
442 to Low Carbonate Clumped Isotope Temperatures in Cryogenician Strata. *AGU*
443 *Advances*, 1(3). doi: 10.1029/2019av000159
- 444 Mackey, T. J., Sumner, D. Y., Hawes, I., & Jungblut, A. D. (2017). Morpholog-
445 ical signatures of microbial activity across sediment and light microenviron-
446 ments of Lake Vanda, Antarctica. *Sedimentary Geology*, 361, 82–92. doi:
447 10.1016/j.sedgeo.2017.09.013
- 448 Mackey, T. J., Sumner, D. Y., Hawes, I., Leidman, S. Z., Andersen, D. T., & Jung-
449 blut, A. D. (2018). Stromatolite records of environmental change in perennially
450 ice-covered Lake Joyce, McMurdo Dry Valleys, Antarctica. *Biogeochemistry*,

- 451 137(1-2), 73–92. doi: 10.1007/s10533-017-0402-1
- 452 Mangenot, X., Gasparri, M., Gerdes, A., Bonifacie, M., & Rouchon, V. (2018). An
453 emerging thermochronometer for carbonate-bearing rocks: $\Delta 47$ /(U-Pb). *Geol-*
454 *ogy*, 46(12), 1067–1070. doi: 10.1130/G45196.1
- 455 Meinicke, N., Ho, S. L., Hannisdal, B., Nürnberg, D., Tripathi, A., Schiebel, R., &
456 Meckler, A. N. (2020). A robust calibration of the clumped isotopes to tem-
457 perature relationship for foraminifers. *Geochimica et Cosmochimica Acta*, 270,
458 160–183. doi: 10.1016/j.gca.2019.11.022
- 459 Müller, I. A., Rodriguez-Blanco, J. D., Storck, J.-C., Santilli, G., Bontognali,
460 T. R. R., Vasconcelos, C., ... Bernasconi, S. M. (2019). Calibration of
461 the oxygen and clumped isotope thermometers for (proto-) dolomite based
462 on synthetic and natural carbonates. *Chemical Geology*, 525, 1–17. doi:
463 10.1016/j.chemgeo.2019.07.014
- 464 Peral, M., Daëron, M., Blamart, D., Bassinot, F., Dewilde, F., Smialkowski, N., ...
465 Waelbroeck, C. (2018). Updated calibration of the clumped isotope thermome-
466 ter in planktonic and benthic foraminifera. *Geochimica et Cosmochimica Acta*,
467 239, 1–16. doi: 10.1016/j.gca.2018.07.016
- 468 Petersen, S. V., Defliese, W. F., Saenger, C., Daëron, M., Huntington, K. W.,
469 John, C. M., ... Winkelstern, I. Z. (2019). Effects of improved ^{17}O cor-
470 rection on interlaboratory agreement in clumped isotope calibrations, esti-
471 mates of mineral-specific offsets, and temperature dependence of acid diges-
472 tion fractionation. *Geochemistry, Geophysics, Geosystems*, 3495–3519. doi:
473 10.1029/2018gc008127
- 474 Piasecki, A., Bernasconi, S. M., Grauel, A. L., Hannisdal, B., Ho, S. L., Leutert,
475 T. J., ... Meckler, N. (2019). Application of clumped isotope thermome-
476 try to benthic foraminifera. *Geochemistry, Geophysics, Geosystems*, 20(4),
477 2082–2090. doi: 10.1029/2018GC007961
- 478 Ross, S. (2003). Peirce’s criterion for the elimination of suspect experimental data.
479 *Journal of Engineering Technology*, 20, 1–12.
- 480 Schauble, E. A., Ghosh, P., & Eiler, J. M. (2006). Preferential formation of ^{13}C
481 – ^{18}O bonds in carbonate minerals, estimated using first-principles lattice
482 dynamics. *Geochimica et Cosmochimica Acta*, 70(10), 2510–2529. doi:
483 10.1016/j.gca.2006.02.011

- 484 Schauer, A. J., Kelson, J., Saenger, C., & Huntington, K. W. (2016). Choice of
485 17O correction affects clumped isotope ($\Delta 47$) values of CO₂ measured with
486 mass spectrometry. *Rapid Communications in Mass Spectrometry*, *30*(24),
487 2607–2616. doi: 10.1002/rcm.7743
- 488 Snell, K. E., Thrasher, B. L., Eiler, J. M., Koch, P. L., Sloan, L. C., & Tabor, N. J.
489 (2013). Hot summers in the Bighorn Basin during the early Paleogene. *Geol-*
490 *ogy*, *41*(1), 55–58. doi: 10.1130/G33567.1
- 491 Wacker, U., Fiebig, J., Tödter, J., Schöne, B. R., Bahr, A., Friedrich, O., . . .
492 Joachimski, M. M. (2014). Empirical calibration of the clumped isotope pale-
493 othemometer using calcites of various origins. *Geochimica et Cosmochimica*
494 *Acta*, *141*, 127–144. Retrieved from 10.1016/j.gca.2014.06.004
- 495 Winkelstern, I. Z., & Lohmann, K. C. (2016). Shallow burial alteration of dolomite
496 and limestone clumped isotope geochemistry. *Geology*, *44*(6), 467–470. doi: 10
497 .1130/G37809.1
- 498 Winograd, I. J., Landwehr, J. M., Coplen, T. B., Sharp, W. D., Riggs, A. C., Lud-
499 wig, K. R., & Kolesar, P. T. (2006). Devils Hole, Nevada, $\delta 18\text{O}$ record ex-
500 tended to the mid-Holocene. *Quaternary Research*, *66*(2), 202–212. doi:
501 10.1016/j.yqres.2006.06.003
- 502 York, D., Evensen, N. M., López, M., & Delgado, J. D. B. (2004). Unified equations
503 for the slope, intercept, and standard errors of the best straight line. *American*
504 *Journal of Physics*, *72*(3), 367–373. doi: 10.1119/1.1632486
- 505 Zaarur, S., Affek, H. P., & Brandon, M. T. (2013). A revised calibration of the
506 clumped isotope thermometer. *Earth and Planetary Science Letters*, *382*, 47–
507 57. Retrieved from <http://dx.doi.org/10.1016/j.epsl.2013.07.026> doi:
508 10.1016/j.epsl.2013.07.026

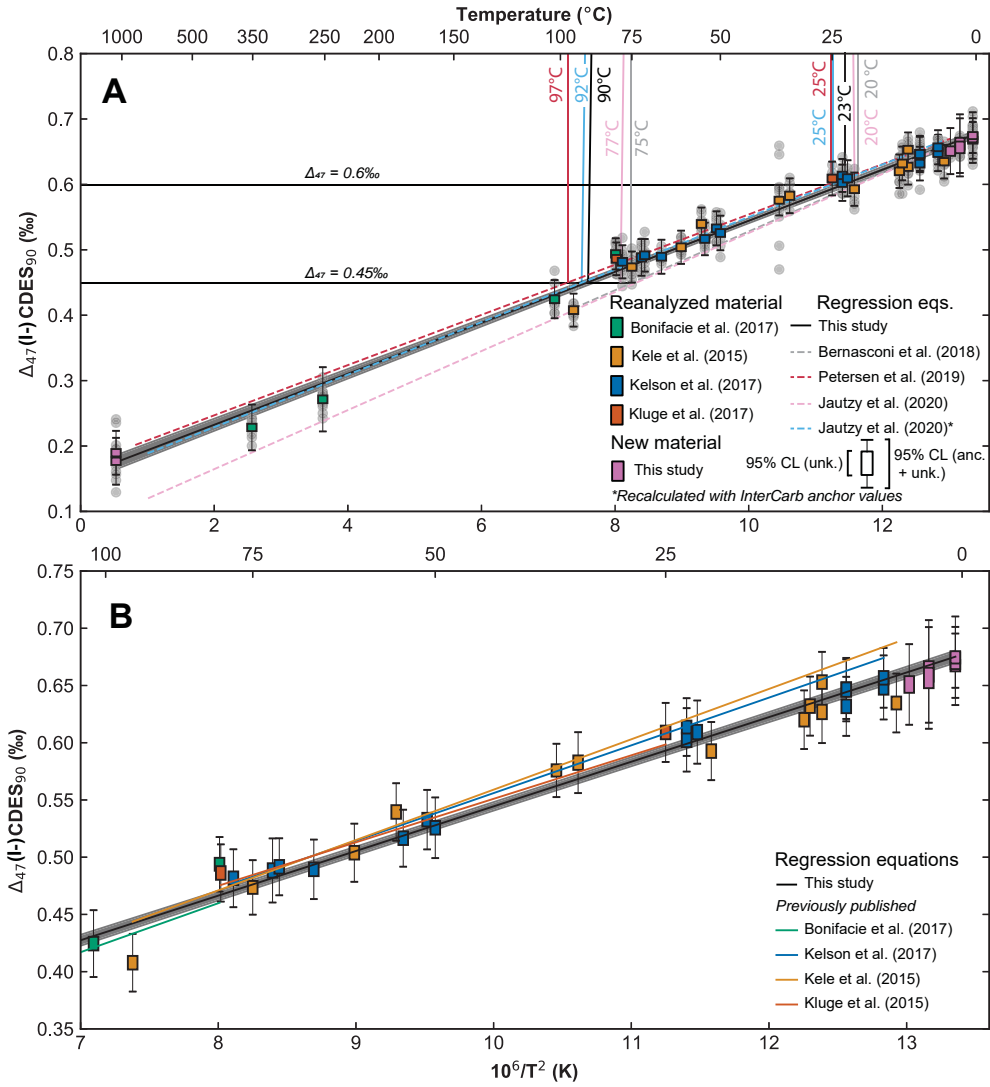


Figure 1. A. Linear $1/T^2$ - Δ_{47} regression and 95% confidence interval (York et al., 2004) for samples (re)analyzed in this study shown with recently published calibrations. Solid vertical lines show approximate formation temperature for each calibration when $\Delta_{47} = 0.45\text{‰}$ and $\Delta_{47} = 0.6\text{‰}$. Error bars correspond to 95% confidence limits accounting for error from unknown and anchor analyses; boxes correspond to 95% CL not accounting for normalization errors. The regression from this study is nearly identical to the regression from Jautzy et al. (2020) when all Δ_{47} values are calculated with 'InterCarb' (Bernasconi et al., submitted) anchor values. B. T- Δ_{47} relationship for samples 0–100°C including regressions from studies with material reanalyzed for this study (Bonifacie et al. (2017), Eq. 1; Kele et al. (2015), Eq. 1; Kelson et al. (2017) Eq. 1; Kluge et al. (2015), Table 1, 'This study, linear fit'; all converted to 90°C acid temperature using AFF values from Petersen et al., 2019).

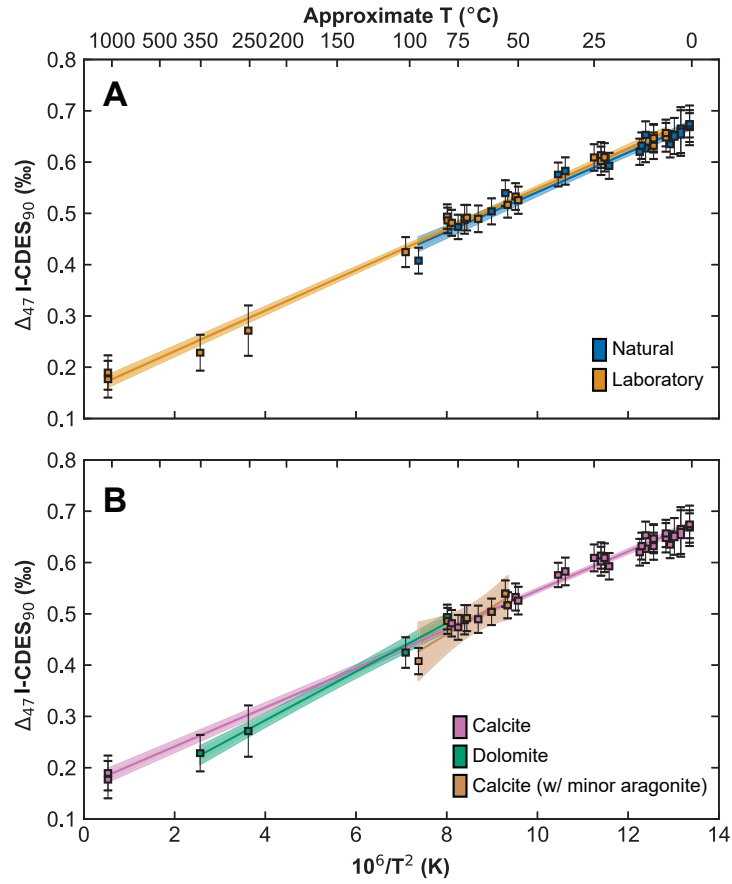


Figure 2. A. $1/T^2$ - Δ_{47} comparison of natural and laboratory precipitated sample material. Error bars correspond to 95% confidence limits accounting for error from both unknown and anchor analyses; boxes correspond to 95% CL not accounting for normalization errors. Natural samples have larger uncertainty of the estimate and a poorer fit, likely due to natural variability in formation temperature and a smaller temperature range. B. Comparison of calcite, (proto)dolomite, and aragonite sample material. The regression lines between calcite and dolomite diverge but 95% confidence intervals overlap; divergence of regression equations may be related to the small temperature range of dolomite (relative to calcite) measured in this study and the small number of dolomite samples.

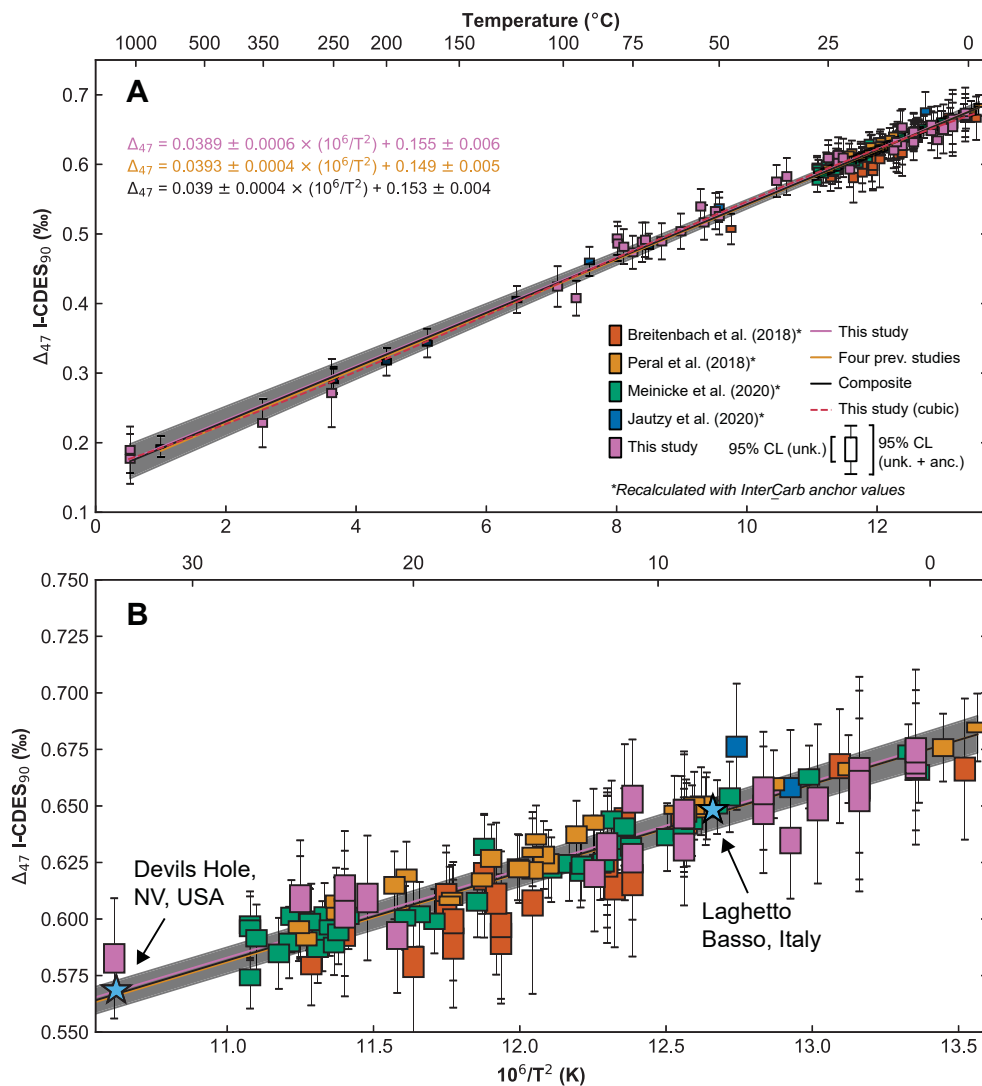


Figure 3. A. All Δ_{47} results from this study shown with data from four recent studies using carbonate-based standardization using laboratory precipitates (Jautzy et al., 2020) and foraminifera (Breitenbach et al., 2018; Peral et al., 2018; Meinicke et al., 2020), recalculated here with InterCarb anchor values (Bernasconi et al., submitted). Error bars correspond to 95% confidence limits accounting for error from both unknown and anchor analyses; boxes correspond to 95% CL not accounting for normalization errors. Regressions through this study (cubic and linear), previous data, and the composite dataset are nearly identical. B. Inset of A from 0–30°C. Slow-growing calcites respectively from Devils Hole, NV, USA, and Laghetto Basso, Italy, measured on an IsoPrime100 at LCSE (see supporting information Text S3) fall directly on the plotted regression lines.